

Postural stability in symmetrical gaits

TERESA ZIELIŃSKA^{1,*}, MACIEJ TROJNACKI²

¹ Institute of Aeronautics and Applied Mechanics (ITLiMS), Warsaw University of Technology, Warsaw, Poland.

² Industrial Research Institute for Automation and Measurements (PIAP), Warsaw, Poland.

In this paper the method of stability analysis of dynamic symmetrical gaits is discussed. The problem of dynamic postural equilibrium, taking into account the role of compliant feet, is solved. The equilibrium conditions are split between the foot attachment points and the points within the foot-end area. The present method is useful for motion synthesis, taking into account robot parameters. It also helps in the robot foot design. As an illustrative example a four-legged diagonal gait is considered. The theoretical results were verified by implementing and observing the diagonal gait in four-legged machine with and without feet.

Key words: walking machines, gait stability, gait synthesis, diagonal dynamic gait

1. Some properties of animal locomotion

The majority of body functions such as beating of the heart, breathing, chewing, locomotion, etc., is periodic [1]. In human walking, synchronized displacement of all main parts of the body is noticeable. Longitudinal and lateral rotation of the trunk, pelvis and twist of shoulders are coordinated with the states of walking cadence (moment of foot touching the ground, foot lift-off, middle stance, etc.) [4], [5]. When the mobility of one joint is affected it influences the motion of the rest. This means that the external disturbance affects the natural rhythm globally and the whole body adapts to it. This also occurs during motion transitions (change from one rhythmic gait to another one) – the changes of leg trajectories are coincident with the motion transition of the other parts of the body. This is evident when looking at the torso. During uphill walk the postural stability is adjusted by changes of torso inclination in the sagittal plane. When the legs are avoiding obstacles the change of

inclination in the frontal plane plays a role. In publications discussing gait biomechanics, the resonant nature of human locomotion is underscored [6].

In general, the periodicity is clearly visible during fast gaits of invertebrate and vertebrate (figure 1). Four legs in eight-legged crabs, three legs in six-legged insects, two legs in quadrupeds during jumps or runs (in the so-called symmetric gaits) are transferred together, they act as one leg in bipeds [3]. The rhythmic gait, when the legs are transferred symmetrically in two groups, is often compared to the oscillations of a single inverted pendulum or spring loaded inverted pendulum. In the recent works, the body is compared not to one pendulum (and moreover not to an inverted one), but to a set of connected pendulums [2]. Using the comparative study of animal leg structure it was shown that the postural adjustment of the whole leg creates a spring effect [7].

Biologically inspired symmetric gaits produce the fastest displacements of walking machines. In hexapod robots, those gaits are statically stable, but in quadrupeds and bipeds, the dynamical effects have a decisive influence on the postural stability. Despite that, the majority of publications devoted to walking

* Corresponding author: Teresa Zielińska, Institute of Aeronautics and Applied Mechanics (ITLiMS), Warsaw University of Technology, ul. Nowowiejska 24, 00-665 Warsaw, Poland. E-mail: teresaz@meil.pw.edu.pl

Received: January 13th, 2009

Accepted for publication: June 12th, 2009

machines focus on the general design problems and on the motion generation principles (e.g., [8], [10]–[12], [14], [17]). The control aspects are also discussed ([21]–[23]), but our detailed research of the analysis of equilibrium conditions in the dynamical gaits, taking into account the stabilizing role of the foot, has not been published yet.

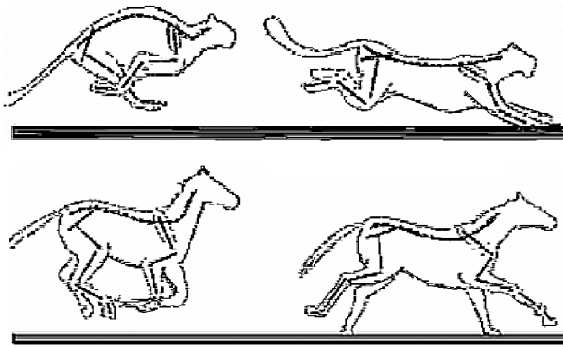


Fig. 1. Examples of symmetrical gaits

The legs of multi-legged walking machines have usually 2 or 3 active degrees of freedom. The additional degrees of freedom (if introduced) are passive. The foot compliance is typically obtained using springs. Many multi-legged robots have feet shaped as balls or as rotating plates [20]. The feet are attached to the shank by passive prismatic joints (figure 2). More complex designs consist of 3 passive DOFs [9]. The potentiometers are sometimes utilized as sensors for monitoring the joint positions (figure 3). The biologically inspired foot with three fingers and 2 active DOFs (figure 4) is a unique example [13] of a more complex structure. In gait synthesis, the attention is paid to the positioning of active joints. The role of foot with its passive DOFs during walk of a multi-legged machine is often neglected.

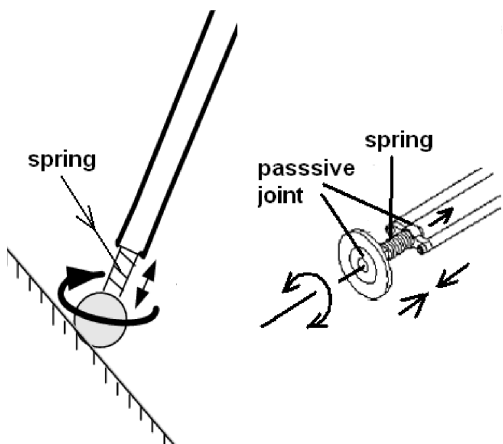


Fig. 2. Foot shaped as a ball or as a plate

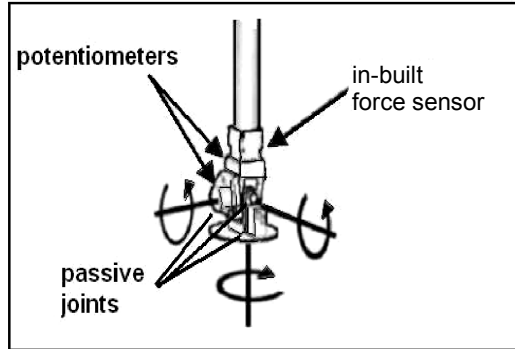


Fig. 3. Leg-end joint with 3 DOFs

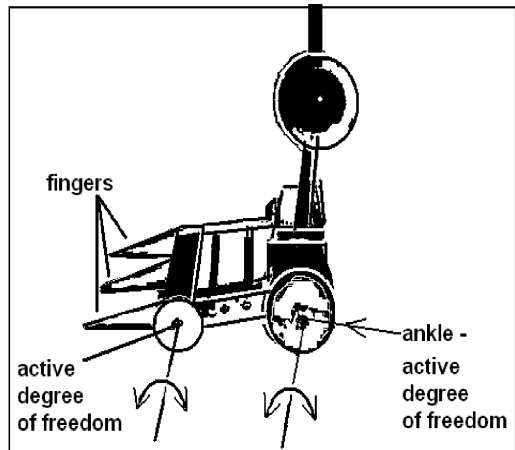


Fig. 4. Scheme of a foot inspired by the structure of an animal foot

2. Problem statement

The foot considered in the example is presented in figure 5. Prismatic joint between the foot and shank is combined with the spring. This endows the leg with compliance – the spring length changes proportionally to the vertical force. This change is small, but produces postural equilibrium as it will be discussed later.

Let us assume that $OXYZ$ is an immobile reference frame, $RXYZ$ is the frame attached to the robot trunk.

The coordinates of the robot mass center ${}^R(xyz)_{CG}$ are equal to:

$${}^R(xyz)_{CG} = \frac{m_0 {}^R(xyz)_0 + \sum_i \sum_j m_{ij} {}^R(xyz)_{ij}}{m}, \quad (1)$$

where: ${}^R(xyz) = \{{}^R_x, {}^R_y, {}^R_z\}$, m_0 – the mass of trunk, $m = m_0 + \sum_i \sum_j m_{ij}$ – the total mass. To illustrate the method we will consider the prototype quadruped

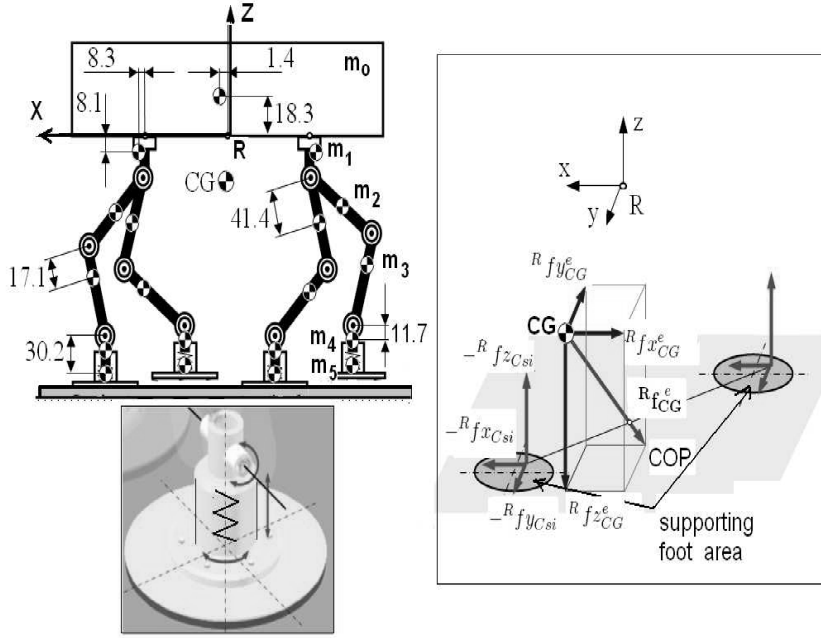


Fig. 5. View of the robot structure, its foot, and the distribution of reaction forces acting on the foot

with dimensions and masses distribution presented in figure 5 (dimensions are expressed in mm). The subscript si indicates the supporting leg.

In the diagonal gait considered, the supporting legs are 1 and 4, or 2 and 3, where 1 denotes the left front leg, 2 – the right front leg, 3 – the left hind leg, 4 – the right hind leg. In further considerations, $s1$ and $s2$ will mark the pair of supporting legs ($s1 = 1$ implies $s2 = 4$, and $s1 = 2$ implies $s2 = 3$). The masses of foot and its mounting parts are equal and are denoted by m_{f4} (mass of foot mounting part), m_{f5} (mass of the foot).

Force equilibrium conditions are usually expressed with reference to the external coordinate frame $OXYZ$. They can easily be expressed with reference to the local frame $RXYZ$ [19]. With reference to the frame $RXYZ$ these conditions are as follows:

$$\begin{aligned} \sum_i {}^R \mathbf{f}_{si} &= \mathbf{F}_e + m({}^R \ddot{\mathbf{r}}_{CG} + {}^R \mathbf{g}) \\ &= \mathbf{F}_e + m_0 {}^R \mathbf{g} + \sum_i \sum_j m_{ij} ({}^R \ddot{\mathbf{r}}_{ij} + {}^R \mathbf{g}) \\ &= \mathbf{F}_e + {}^R \mathbf{f}_{CG} = [{}^R f_{xCG}^e, {}^R f_{yCG}^e, {}^R f_{zCG}^e]^T, \end{aligned} \quad (2)$$

where ${}^R \mathbf{g} = {}^R T_O [0, 0, -g]^T$, \mathbf{g} is the gravity constant. ${}^R T_O$ is the transformation matrix from $OXYZ$ to $RXYZ$. ${}^R \mathbf{f}_{CG}$ is the resultant force vector acting on the robot mass center. ${}^R \mathbf{F}_{si} = [{}^R f_{xsi}, {}^R f_{ysi}, {}^R f_{zsi}]^T$ is the vector of force exerted by the leg-end. The torque equilibrium conditions expressed with reference to the frame $RXYZ$ are:

$$\begin{aligned} &\sum_i ({}^R \mathbf{r}_{si} - {}^R \mathbf{r}_{CG}) \times {}^R \mathbf{f}_{si} \\ &= \sum_i ({}^R \mathbf{r}_{si} - {}^R \mathbf{r}_{CG}) \times (\mathbf{F}_e + m({}^R \ddot{\mathbf{r}}_{CG} + {}^R \mathbf{g})) \\ &= \sum_i ({}^R \mathbf{r}_{si} - {}^R \mathbf{r}_{CG}) \times (\mathbf{F}_e + {}^R \mathbf{f}_{CG} \\ &= [-{}^R \mathbf{M}_x^e - {}^R \mathbf{M}_y^e, -{}^R \mathbf{M}_z^e]^T. \end{aligned} \quad (3)$$

${}^R \mathbf{M}_x^e$, ${}^R \mathbf{M}_y^e$, ${}^R \mathbf{M}_z^e$ are the external moments applied to the robot. In our considerations, we assume only the rotation about the vertical axis Z passing through the point R ; I_{zz} is the main inertia moment around the axis Z , and ϕ_Z is the rotation angle. With the above assumption: ${}^R \mathbf{M}_x^e = 0$, ${}^R \mathbf{M}_y^e = 0$, ${}^R \mathbf{M}_z^e = I_{zz} \ddot{\phi}_Z$. Stating this more briefly, we denote $\mathbf{F}_e + {}^R \mathbf{f}_{CG}$ by ${}^R \mathbf{f}_{CG}^e$

$$\mathbf{Af} = \mathbf{F}, \quad (4)$$

where

$$\mathbf{A} = \begin{bmatrix} 1 & 0 & 0 & 1 & 0 & 0 \\ 0 & 1 & 0 & 0 & 1 & 0 \\ 0 & 0 & 1 & 0 & 0 & 1 \\ 0 & -{}^R z_{s1} & {}^R y_{s1} & 0 & -{}^R z_{s2} & {}^R y_{s2} \\ {}^R z_{s1} & 0 & -{}^R x_{s1} & {}^R z_{s2} & 0 & -{}^R x_{s2} \\ -{}^R y_{s1} & {}^R x_{s1} & 0 & -{}^R y_{s2} & {}^R x_{s2} & 0 \end{bmatrix},$$

$$\mathbf{f} = [{}^R f_{xsi}, {}^R f_{ysi}, {}^R f_{zsi}, {}^R f_{xsi}, {}^R f_{ysi}, {}^R f_{zsi}]^T,$$

$$\begin{aligned} \mathbf{F} &= [{}^R f_{x_{CG}}^e, {}^R f_{y_{CG}}^e, {}^R f_{z_{CG}}^e, {}^R M_x, {}^R M_y, {}^R M_z]^T, \\ {}^R M_x &= -{}^R f_{y_{CG}}^e {}^R z_{CG} + {}^R f_{z_{CG}}^e {}^R y_{CG}, \\ {}^R M_y &= {}^R f_{x_{CG}}^e {}^R z_{CG} - {}^R f_{z_{CG}}^e {}^R x_{CG}, \\ {}^R M_z &= -{}^R f_{x_{CG}}^e {}^R y_{CG} + {}^R f_{y_{CG}}^e {}^R x_{CG} - I_{zz} \ddot{\phi}_z. \end{aligned} \quad (5)$$

The matrix \mathbf{A} is singular ($\text{rank}(\mathbf{A}) < 6$), the rank of the extended matrix is 6 which means that the equalities cannot be fulfilled. The equilibrium conditions described by (2), (3) cannot be fulfilled considering only the leg-ends. Taking into account the stabilizing role of the feet we split the equilibrium conditions between the points B_i and C_i for two supporting legs. Passive joint in the foot attachment allows the rotation about the axis parallel to Y , but not the rotation about the X direction. Therefore we assume that the forces exerted at points B_{si} of the supporting legs compensate for the moment ${}^R M_x$. For the evaluation of vertical leg-end forces we assume that the points B_i are located at a constant distance $H - h$ from the plane RXY (${}^R z_{Bsi} = -H + h$).

Taking into account the forces equilibrium condition and the moment ${}^R M_x$ (the 2nd and 4th equality in (4)) we obtain the forces ${}^R f_{z_{Bsi}}$:

$$\begin{aligned} {}^R f_{z_{Bsi}} &= \frac{{}^R f_{y_{CG}}^e (-{}^R z_{CG} + h - H)}{{}^R y_{Bsi1} - {}^R y_{Bsi2}} \\ &+ \frac{({}^R f_{z_{CG}}^e - 2(m_{f4} + m_{f5})g)({}^R y_{CG} - {}^R y_{Bsi2})}{{}^R y_{Bsi1} - {}^R y_{Bsi2}}, \\ {}^R f_{z_{Bsi}} &= {}^R f_{z_{CG}}^e - 2(m_{f4} + m_{f5})g - {}^R f_{z_{Bsi}}. \end{aligned} \quad (6)$$

Having known those components of vertical force exerted at the points B_i the change of the spring length dh_i under the loads ${}^R f_{z_{Bsi}}$ can be evaluated:

$$\begin{aligned} dh_1 &= \frac{|{}^R f_{z_{Bsi1}}|}{k_1}, \\ dh_2 &= \frac{|{}^R f_{z_{Bsi2}}|}{k_2}, \end{aligned} \quad (7)$$

k_1, k_2 are the spring constants. The heights of the points B_{si} are equal to $h_1 = h - dh_1$ and $h_2 = h - dh_2$.

Having the above result we express separately the moments ${}^R M_x^{Bsi}$, ${}^R M_y^{Bsi}$ acting on CG due to the forces at B_{si} :

$$\begin{aligned} {}^R M_x^{Bsi} &= {}^R f_{y_{Bsi}} H + {}^R f_{z_{Bsi}} ({}^R y_{Bsi1} - {}^R y_{CG}), \\ {}^R M_y^{Bsi} &= -{}^R f_{x_{Bsi}} H - {}^R f_{z_{Bsi}} ({}^R x_{Bsi1} - {}^R x_{CG}). \end{aligned} \quad (8)$$

The leg-end reaction forces ($-{}^R f_{x_{Csi}}, -{}^R f_{y_{Csi}}, -{}^R f_{z_{Csi}}$) are applied at the points C_{si} (figure 6). Those points are by h_i lower than B_{si} and are translated by dx_{si} dy_{si} towards the vertical projection of B_i onto the supporting plane (${}^R x_{Csi} = {}^R x_{Bsi} + dx_{si}$, ${}^R y_{Csi} = {}^R y_{Bsi} + dy_{si}$). The moments ${}^R M_x^{Csi}$, ${}^R M_y^{Csi}$ exerted in CG due to the forces at C_{si} are equal to:

$$\begin{aligned} {}^R M_x^{Bsi} &= {}^R f_{y_{Csi}} (H + h_i) \\ &+ {}^R f_{z_{Csi}} (dy_{si} + {}^R y_{Bsi1} - {}^R y_{CG}), \\ {}^R M_y^{Csi} &= -{}^R f_{x_{Csi}} (H + h_i) \\ &- {}^R f_{z_{Csi}} (dx_{si} + {}^R x_{Bsi1} - {}^R x_{CG}). \end{aligned} \quad (9)$$

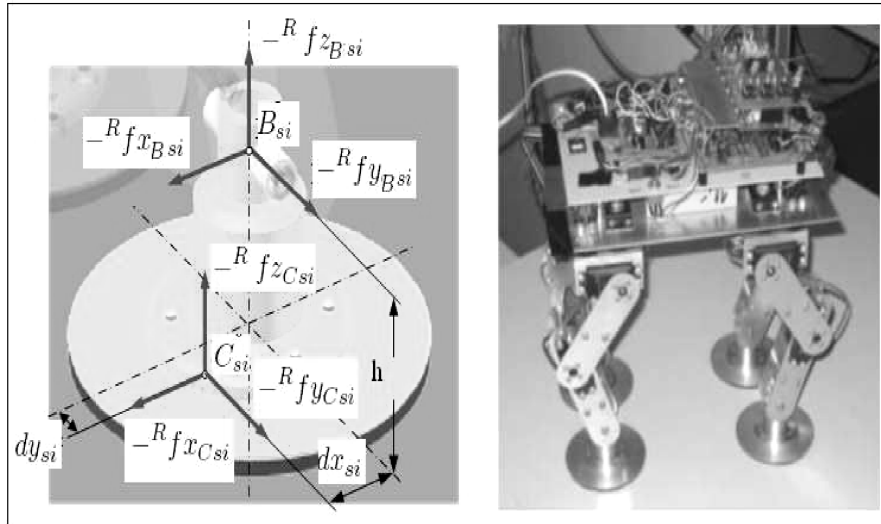


Fig. 6. Left: robot foot and notation, right: view of the prototype

We keep in mind that ${}^R f z_{Csi} = {}^R f z_{Bsi} + (m_{f4} + m_{f5})g$, ${}^R f x_{Csi} = {}^R f x_{Bsi}$, ${}^R f y_{Csi} = {}^R f y_{Bsi}$. We assume that the points C_i are so located that in the feet mounting points B_i additional moments around X and Y directions are not produced, therefore the moments expressed by (8) are equal to the moments (9):

$$\begin{aligned} {}^R M_x^{Bsi} &= {}^R M_x^{Csi}, \\ {}^R M_y^{Bsi} &= {}^R M_y^{Csi}. \end{aligned} \quad (10)$$

First the moments ${}^R M_x^{Bsi}$, ${}^R M_x^{Csi}$ are compared taking into account (8) and (9), ${}^R f y_{Cs1}$ is evaluated for $i = 1$, and the result is used in (10) for $i = 2$ taking into account ${}^R F y_{Cs2} = {}^R f y_{CG}^e - {}^R F y_{Cs1}$. After regrouping the terms the relationship between dy_1 and dy_2 is as follows:

$$\begin{aligned} dy_1 &= a_1 - b_1 dy_2 - d_1 + c_1, \\ a_1 &= \frac{h_1({}^R y_{CG} - {}^R y_{Bs2})g(m_{f4} + m_{f5})}{h_2 {}^R f z_{Cs1}}, \\ b_1 &= \frac{h_1 {}^R f z_{Cs2}}{h_2 {}^R f z_{Cs1}}, \\ d_1 &= \frac{h_1 {}^R f y_{CG}^e}{{}^R f z_{Cs1}}, \\ c_1 &= \frac{({}^R y_{CG} - {}^R y_{Bs1})g(m_{f4} + m_{f5})}{{}^R f z_{Cs1}}. \end{aligned} \quad (11)$$

Analogically the moments ${}^R M_y^{Bsi}$, ${}^R M_y^{Csi}$ are compared and the relationship between dx_1 and dx_2 is obtained:

$$\begin{aligned} dx_1 &= -aa_1 + bb_1 dx_2 + dd_1 - cc_1, \\ aa_1 &= \frac{h_1({}^R x_{CG} - {}^R x_{Bs2})g(m_{f4} + m_{f5})}{h_2 {}^R f z_{Cs1}}, \\ bb_1 &= \frac{h_1 {}^R f z_{Cs2}}{h_2 {}^R f z_{Cs1}}, \\ dd_1 &= \frac{h_1 {}^R f x_{CG}^e}{{}^R f z_{Cs1}}, \\ cc_1 &= \frac{({}^R x_{CG} - {}^R x_{Bs1})g(m_{f4} + m_{f5})}{{}^R f z_{Cs1}}. \end{aligned} \quad (12)$$

Let us define ${}^R COP$ – the intersection point of ${}^R f_{CG}$ with the supporting plane (figure 5). This point is

also the attachment point of the resultant reaction force vector. During the real (physical) walk it is also the Center Of Pressure (COP). In smooth walk (with smooth motion of the trunk), it is expected that ${}^O z_{COP} = {}^R z_{COP} = -H = \text{const}$. The point COP being the intersection of the vector ${}^R f_{CG}$ with the plane ${}^R z_{COP} = -H$ has the following coordinates:

$${}^R x_{COP} = {}^R x_{CG} - \frac{{}^R f x_{CG}}{{}^R f z_{CG}}(H + {}^R z_{CG}), \quad (13)$$

$${}^R y_{COP} = {}^R y_{CG} - \frac{{}^R f y_{CG}}{{}^R f z_{CG}}(H + {}^R z_{CG}). \quad (14)$$

In stable posture, the moments ${}^R M_x$, ${}^R M_y$ resulting from the reaction forces and evaluated in the supporting plane in relation to the reference point COP shall be equal to zero:

$$\begin{aligned} {}^R M x_{COP} &= ({}^R y_{Cs1} - {}^R y_{COP}) {}^R f z_{Cs1} \\ &+ ({}^R y_{Cs2} - {}^R y_{COP}) {}^R f z_{Cs2} = 0, \end{aligned} \quad (15)$$

$$\begin{aligned} {}^R M y_{COP} &= ({}^R x_{Cs1} - {}^R x_{COP}) {}^R f z_{Cs1} \\ &+ ({}^R x_{Cs2} - {}^R x_{COP}) {}^R f z_{Cs2} = 0. \end{aligned} \quad (16)$$

Considering (15), (16) and the 3rd equality from (4) we obtain:

$$\begin{aligned} {}^R f z_{Cs1} &= \frac{{}^R f z_{CG}^e ({}^R y_{COP} - {}^R y_{Cs2})}{{}^R y_{Cs1} - {}^R y_{Cs2}} \\ &= \frac{{}^R f z_{CG}^e ({}^R y_{COP} - {}^R y_{Bs2} - dy_{s2})}{{}^R \Delta y_{Bs1} + dy_{s1} - dy_{s2}}, \end{aligned} \quad (17)$$

$$\begin{aligned} {}^R f z_{Cs1} &= \frac{{}^R f z_{CG}^e ({}^R x_{COP} - {}^R x_{Cs2})}{{}^R x_{Cs1} - {}^R x_{Cs2}} \\ &= \frac{{}^R f z_{CG}^e ({}^R x_{COP} - {}^R x_{Bs2} - dx_{s2})}{{}^R \Delta x_{Bs1} + dx_{s1} - dx_{s2}}, \end{aligned}$$

where ${}^R \Delta x_{Bs1} = {}^R x_{Bs1} - {}^R x_{Bs2}$, ${}^R \Delta y_{Bs1} = {}^R y_{Bs1} - {}^R y_{Bs2}$.

Remembering that on the basis of (6) the forces ${}^R f z_{Cs1} ({}^R f z_{Cs1} = {}^R f z_{Bs1} + g(m_{f4} + m_{f5}))$ are known, we rearrange each equation (17) separately:

$$\begin{aligned} dy_{s1} &= \frac{{}^R f z_{CG}^e ({}^R y_{COP} - {}^R y_{Bs2})}{{}^R f z_{Cs1}} - {}^R \Delta y_{Bs1} \\ &- dy_{s2} \frac{{}^R f z_{Cs2}}{{}^R f z_{Cs1}} = a_y - dy_{s2} \frac{{}^R f z_{Cs2}}{{}^R f z_{Cs1}}, \end{aligned} \quad (18)$$

$$\begin{aligned} dx_{s1} &= \frac{^R f z_{CG} (^R x_{COP} - ^R x_{Bs2})}{^R f z_{Cs1}} - ^R \Delta x_{Bs1} \\ -dx_{s2} \frac{^R f z_{Cs2}}{^R f z_{Cs1}} &= a_x - dx_{s2} \frac{^R f z_{Cs2}}{^R f z_{Cs1}}. \end{aligned} \quad (18)$$

Now the results (18) are inserted into (11) and (12), which produces:

$$\begin{aligned} dy_2 &= \frac{a_y + d_1 - a_1 - c_1}{^R f z_{Cs2} - b_1}, \\ dx_2 &= \frac{a_x + dd_1 + aa_1 + cc_1}{^R f z_{Cs2} + bb_1}. \end{aligned} \quad (19)$$

Once dx_i , dy_i are obtained the remaining force components can easily be calculated using (10).

3. Verification of the method

The experimental confirmation of the role of the feet in postural stabilization was obtained by observing stable displacement of the walking machine by using the diagonal gait. After dismounting the feet the machine overturned when trying to move by that gait. This proves that the stable posture is obtained due to the shift of leg-end force vector within the sole area as it was predicted and discussed above. The method was validated by simulation where the parameters of real robot and its gait were taken into account. Robot structure and its mass distribution are presented in figure 5. The legs have 3 active DOFs – 2 in the hip and 1 in the knee. As was mentioned, the shank and foot are connected by a passive joint. The attachment uses an in-built vertical spring (figure 6). The robot and its control system were described in [15], [16], and in [18] the motion properties were discussed. The robot trunk length l_0 equals 0.25 [m]; width, $w_0 = 0.18$ [m]; thigh and shank lengths, $l_2 = l_3 = 0.08$ [m]; total mass, $m = 2.522$ [kg]; trunk mass, $m_0 = 1.382$ [kg]; mass of hip segment, $m_{11} = m_1 = 0.094$ [kg]; mass of thigh, $m_{12} = m_2 = 0.034$ [kg]; mass of shank, $m_{13} = m_3 = 0.08$ [kg]; foot masses: the upper part, $m_{f4} = 0.017$ [kg], the lower part, $m_{f5} = 0.06$ [kg].

The results obtained for the robot moving along a straight line with constant speed are presented. The robot height was $H = 0.22$ [m], the step length was 0.2 [m] and the walking speed was 0.083 [m/s], the

spring constants were $k_1 = k_2 = 580$ N/cm. The results are presented in figures 7 to 9. Figure 7 illustrates dx_1 shift and dx_2 shifts for a pair of supporting legs, and figure 8 shows dy_i shifts. The side shifts dy_i of the points C_{si} are very small, the forward–backward dx_i shifts are bigger, but the plate type feet with the radius not smaller than 3 cm will assure the postural stability.

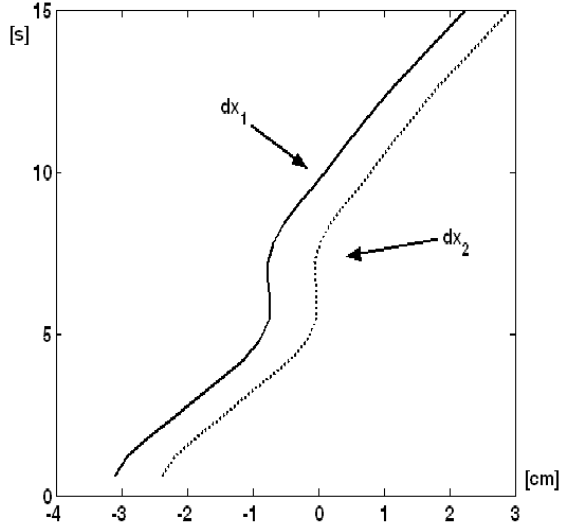


Fig. 7. dx_1 shift (front leg) and dx_2 shift (hind leg)

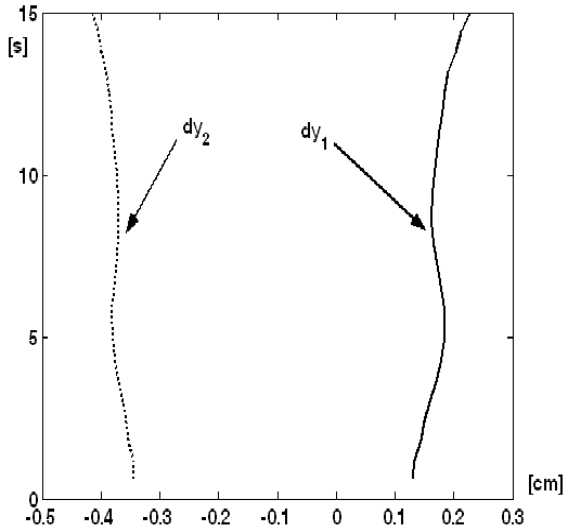


Fig. 8. dy_1 shift (front leg) and dy_2 shift (hind leg)

In figures 9 and 10, the vertical components of reaction forces at the points B_{si} are shown. Figure 11 presents the sum of those forces. For better illustration the forces were normalized by the absolute value of the body weight (without the weight of the 2 supporting feet) and expressed in per cent. The hind leg in that gait is loaded more than the front one. The impact visible for the front leg force, at the beginning

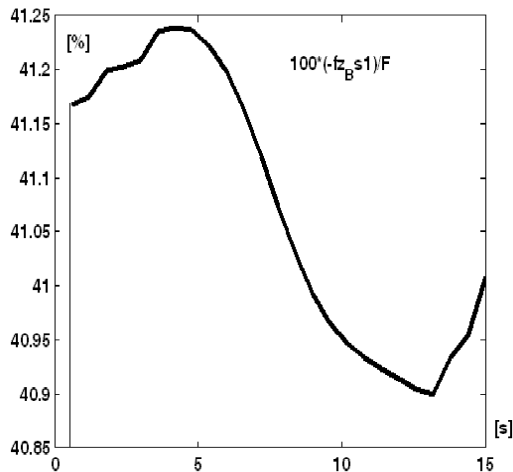


Fig. 9. Vertical component of the reaction force at point B of the front leg

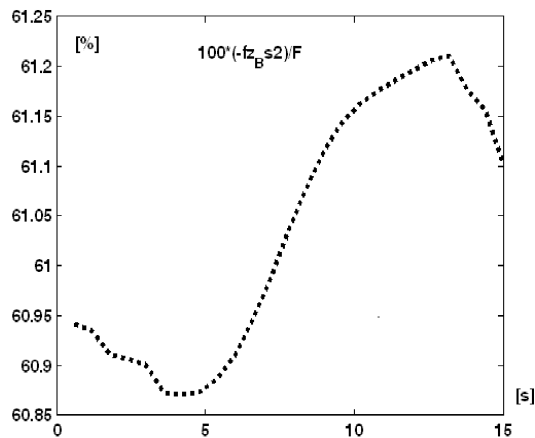


Fig. 10. Vertical component of the reaction force at point B of the hind leg

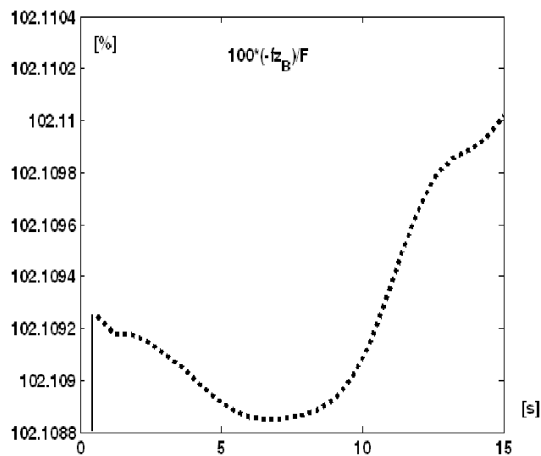


Fig. 11. Vertical component of the sum of the reaction forces

of the support phase, suggests that the front leg stabilizes the body posture when the body tends to rotate to the side of that leg about the diagonal connecting the hips of the previous supporting pair. The substantial

impact at the end of the support phase of the hind leg shows that this leg produces stronger lift-off impulse pushing the body. Similar properties were observed in the gaits of horses, but no calculations have been provided [7]. The shape of the time plot of force in figure 11 resembles that of the reaction force registered during human walk (figure 12). At the beginning and the end of the support phase, force impacts are visible, the impact at the end of the support phase is relatively stronger than that at the beginning. The average impact (above the body weight) is weak, i.e. within 2 per cent.

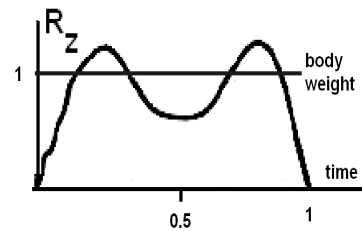


Fig. 12. Vertical component of the reaction force during human walk

4. Conclusion

The confirmation that the feet play an important role in postural stabilization of a walking machine using a diagonal gait has been obtained. The present method of force evaluation decomposes equilibrium conditions taking into account foot attachments and foot-ends. Disregarding the condition for ${}^R M_z$ makes the rotation of the feet around the Z axis possible. In the considered prototype (as in the majority of quadrupeds), the feet rotate freely around the vertical axis passing through the point of their attachment to the shank. Due to the existence of this freedom of motion about the vertical axis in real robots the fact that no condition has been imposed on M_z becomes a logical consequence.

Postural stability observed during motion of a real machine using the diagonal gait confirms the correctness of the present considerations. The relations obtained are useful for the walking machine design. The knowledge of leg-end force application point displacements dx_{si} , dy_{si} towards the feet mounting points has an important influence on the synthesis of dynamical stable gaits. The knowledge of those displacements is needed to assess whether the foot supporting area will assure postural stability. On the basis on the present results the change of the foot area or the change of the leg configuration (change in the position of CG) can be used for postural stabilization.

Acknowledgement

The authors gratefully acknowledge the support for this work from Warsaw University of Technology Research Program and the Ministry of Scientific Research and Information Technology, Grant N N514 297935.

References

- [1] BUCHLI J., RIGHETTI L., IJSPEERT A.J., *Engineering Entrainment and Adaptation in Limit Cycle Systems. From Biological Inspiration to Application in Robotics*, Biological Cybernetics, 2006, Vol. 95, 645–664.
- [2] FISCHER M.S., WITTE H.F., *Evolution of Vertebrate Locomotory System. Walking: Biological and Technological Aspects*, CISM Courses and Lectures, No. 467, Pfeiffer F., Zielińska T. (editors), Springer, 2004, 51–80.
- [3] FULL R.J., *Invertebrate locomotor system*, [in:] *Handbook of Computation Physiology*, Danzler W. (editor), Oxford University Press, 1997, 853–930.
- [4] VAUGHAN CH.L. DAVIS B.L., O'CONNOR J.C., *Dynamics of Human Gait*, Human Kinetics Publishers, 1992.
- [5] WINTER D.A., *Biomechanics and Motor Control of Human Gait: Normal, Elderly and Pathological*, University of Waterloo, 1991.
- [6] ZIELIŃSKA T., *Coupled Oscillators Utilised as Gait Rhythm Generators of a Two-Legged Walking Machine*, Biological Cybernetics, 1996, 74, 263–273.
- [7] ZIELIŃSKA T., *Biological Aspects of Locomotion. Walking: Biological and Technological Aspects*, CISM Courses and Lectures, No. 467, Pfeiffer F., Zielińska T. (editors), Springer, 2004, 1–30.
- [8] GARDNER J.F., *Efficient Computation of Force Distribution for Walking Machines on Rough Terrain*, Robotica, 1992, 10 (5), 427–433.
- [9] GARCIA E., GALVEZ J.A., GONZALEZ de SANTOS P., *On Finding the Relevant Dynamics for Model-Based Controlling Walking Robots*, Journal of Intelligent and Robotic Systems, 2003, Vol. 37, issue 4, 375–398.
- [10] KLEIN C.A., KITTIVATCHARAPONG S., *Optimal Force Distribution for the Legs of a Walking Machine with Friction Cone Constraints*, IEEE Trans. on Robotics and Automation, 1990, 6 (1), 73–85.
- [11] MARTINS-FILHO L.S., PRAJOUX R., *Locomotion Control of a Four-legged Robot Embedding Real-time Reasoning in the Force Distribution*, Robotics and Autonomous Systems, 2000, 32, 219–235.
- [12] PFEIFFER F., ELTZE J., WEIDEMANN H.J., *Six-legged Walking Considering Biological Principles*, Robotics and Autonomous Systems, 1995, Vol. 14, 223–232.
- [13] SPENNEBERG D., ALBRECHT M., BACKHAUS T., HILLJEGERDES J., KIRCHNER F., STRACK A., SCHENKER H., *Aramies: a Four-legged Climbing and Walking Robot*, Proc. of 8th International Symposium iSAIRAS, Munich, September 2005 (CD ROM).
- [14] TAKEMURA H., DEGUCHI M., UEDA J., MATSUMOTO Y., OGASAWARA T., *Slip-adaptive Walk of Quadruped Robot*, Robotics and Autonomous Systems, 2005, 53, 124–141.
- [15] TROJNACKI M., *Motion Description of Quadruped Robot* (in Polish), [in:] *Zeszyty Naukowe Politechniki Rzeszowskiej*, 2005, No. 222, 357–364.
- [16] TROJNACKI M., *The Modeling, Programming and Computer Simulation of Motion for a Four-legged Robot*, [in:] *Projektowanie Mechatroniczne*, Uhl T. (editor), Wydawnictwo Instytutu Technologii Eksploatacji PIB, Krakow, 2006, 149–160.
- [17] ZHOU D., LOW K.H., ZIELIŃSKA T., *An Efficient Foot-force Distribution Algorithm for Quadruped Walking Robots*, Robotica, 2000, Vol. 18, 403–413.
- [18] ZIELIŃSKA T., TROJNACKI M., *Motion Synthesis of Dynamically Stable Two-legged Gait for a Quadruped Robot, Theoretical Considerations* (in Polish), (1), PAR 11/2007, 5–11.
- [19] ZIELIŃSKA T., *Walking Machines: Fundamentals, Design, Control and Biological Patterns* (in Polish), PWN, 2003.
- [20] ZIELIŃSKA T., HENG J., *Mechanical Design of Multifunctional Quadruped*, Mechanism and Machine Theory, 2003, Vol. 38, 463–478.
- [21] ZIELIŃSKA T., *Motion Synthesis*, [in:] *Walking: Biological and Technological Aspects*, CISM Courses and Lectures, No. 467, Pfeiffer F., Zielińska T. (editors), Springer-Verlag, 2004, 151–187.
- [22] ZIELIŃSKA T., *Control and Navigation Aspects of a Group of Walking Robots*, Robotica, Cambridge University Press, 2006, Vol. 24, 23–29.
- [23] ZIELIŃSKA T., HENG J., *Real-time Control System for a Group of Autonomous Walking Robots*, Advanced Robotics, 2006, Vol. 20, No. 5, 543–561.